

Lawrence Berkeley National Laboratory

Recent Work

Title

DAMAGE OF ZEOLITE Y IN THE TEM AND ITS EFFECTS ON TEM IMAGES

Permalink

<https://escholarship.org/uc/item/4v4348b7>

Authors

Csencsits, R.

Gronsky, R.

Publication Date

1987



Lawrence Berkeley Laboratory

UNIVERSITY OF CALIFORNIA

Materials & Chemical Sciences Division

RECEIVED
LAWRENCE
BERKELEY LABORATORY

APR 22 1987

Center for Advanced Materials

LIBRARY AND
DOCUMENTS SECTION

Submitted to Ultramicroscopy

DAMAGE OF ZEOLITE Y IN THE TEM AND ITS EFFECTS ON TEM IMAGES

R. Csencsits and R. Gronsky

January 1987

TWO-WEEK LOAN COPY
*This is a Library Circulating Copy
which may be borrowed for two weeks*



*LBL-22695
e-2*

DISCLAIMER

This document was prepared as an account of work sponsored by the United States Government. While this document is believed to contain correct information, neither the United States Government nor any agency thereof, nor the Regents of the University of California, nor any of their employees, makes any warranty, express or implied, or assumes any legal responsibility for the accuracy, completeness, or usefulness of any information, apparatus, product, or process disclosed, or represents that its use would not infringe privately owned rights. Reference herein to any specific commercial product, process, or service by its trade name, trademark, manufacturer, or otherwise, does not necessarily constitute or imply its endorsement, recommendation, or favoring by the United States Government or any agency thereof, or the Regents of the University of California. The views and opinions of authors expressed herein do not necessarily state or reflect those of the United States Government or any agency thereof or the Regents of the University of California.

Damage of Zeolite Y in the TEM and its Effects on TEM Images

R. Csencsits and R. Gronsky

National Center for Electron Microscopy
Center for Advanced Materials
Lawrence Berkeley Laboratory
University of California
Berkeley, CA 94720

ABSTRACT

Electron diffraction has been used to study the vitrification of Y zeolite in the transmission electron microscope (TEM). Calculations and experimental evidence have confirmed that in the range 80-200kV, the damage of Y zeolites is radiolytic in the TEM. Incident beam electrons interact with specimen electrons which leads to a rearrangement of the structure. The proposed mechanism for this transformation involves enhancement of structural relaxation at Al sites due to the presence of a charge compensating cation.

Computer image simulation was used to assess the effects of damage on high resolution electron microscope (HREM) images of Y zeolites. Simulated images of perfect Y zeolite revealed that only for a specimen 10-20nm thick would the HREM image be a structure image at Scherzer defocus (-60nm); at thickness greater than 20nm the images contain non-structural detail due to second order interferences. At larger defocus values (-100nm), thicker crystals (60nm) "with 30-50% of their thickness amorphous" produce images which can be related to the structure because the presence of the amorphous material decreases the visibility of the non-structural detail.

Damage of Zeolite Y in the TEM and its Effects on TEM Images

R. Csencsits and R. Gronsky

National Center for Electron Microscopy
Center for Advanced Materials
Lawrence Berkeley Laboratory
University of California
Berkeley, CA 94720

INTRODUCTION

High resolution electron microscopy (HREM) is a valuable technique for studying catalyst systems because it gives direct information about the structure and the types and distribution of defects present in the structure. The vitrification of zeolites (and other silicates) during observation in the transmission electron microscope (TEM) has been well documented.¹⁻⁶ Observations show that the damage rate of zeolites depends on the Si/Al-ratio, on the size of the cations,² and on the extent of hydration.¹ This work is a systematic investigation of the damage of zeolite Y in the TEM; the goals of this study are to propose a mechanism for damage of zeolite Y in the TEM and to access the effects of damage on HREM images using computer simulation.

The types of damage possible in an electron microscope can be classified under two general headings: knock-on and radiolytic. "Knock-on" damage involves the interaction of the incident electron with the core of an atom in the specimen. An atom is "knocked" from its site, thereby changing the structure. Radiolytic damage involves the transfer of energy from the incident electron to the electrons in the specimen. The increase in energy of the specimen electrons results in bond breakage and consequently the possible alteration of the structure.

Knock-on Damage

The cross-section for direct interaction of the probing electron and the nuclear core of an atom in the specimen is called the knock-on cross-section. For relativistic electrons this cross-section is given by^{7,8}

$$\sigma_n = \left\{ \frac{4\pi a_0^2 U_R^2}{(mc^2)^2} \right\} \left\{ \frac{Z^2(1-\beta^2)}{\beta^4} \right\} \left\{ \left(\Omega_r \right) + 2\pi\alpha\beta \left(\Omega_r \right)^{1/2} - (\beta^2 + \pi\alpha\beta) \ln \left(\Omega_r \right) - 1 - 2\pi\alpha\beta \right\} \quad (1)$$

where:

$$\Omega_r = \frac{T_{\max}}{T_{\text{th}}} \quad T_{\max} = \frac{2 U_p (U_p + 2mc^2)}{Mc^2}$$

$$\beta = \left\{ 1 - \frac{1}{\left(\frac{U_p}{mc^2} + 1 \right)^2} \right\}^{1/2}$$

U_p is the incident beam kinetic energy (keV), and mc^2 is the rest energy of the electron (511 keV). Mc^2 is the rest energy of the nucleus, α is $Z/137$, Z is the atomic number, U_R is the Rydberg constant (0.0136 keV), and a_0 is the Bohr radius (0.053 nm). The maximum energy that an incident electron can transfer to a nucleus is T_{\max} . The minimum energy necessary to move an atom off its lattice site into some metastable position is T_{th} , which depends directly on the atomic number.

All materials undergo direct displacement of atoms above their specific threshold energy. Above the threshold energy for the knock-on process, the cross-section for knock-on increases with increasing accelerating voltage. The potential damage due to electron-nuclear interaction becomes more severe as the incoming electron gets more and more energetic. At higher accelerating voltages the electron has enough energy to cause multiple damage events. The quantity, $N_d = \frac{T_{\max}}{2 T_{\text{th}}}$, takes into account the possible cascade of damage events. The knock-on damage cross-section includes the cross-section for displacement of an atom directly due to interaction with the electron wave and the probability of being displaced by another "knocked" atom, i.e., $\sigma_{\text{kd}} = \sigma_n \times N_d$. Its variation with accelerating voltage is shown for aluminum in zeolite Y in figure 1.

Radiolytic Damage

The relativistic cross-section for the interaction between the incident electron and the specimen electron is given by⁹

$$\sigma_e = \left(\frac{8 \pi a_0^2 U_R^2}{mc^2} \right) \left(\frac{Z}{T'_{\text{th}} \beta^2} \right) \quad (2)$$

where: T'_{th} is the minimum energy that must be transferred to the electrons of the solid to produce atomic nuclear movement, Z is the number of electrons (usually the atomic number) belonging to the target atom, and a_0 , U_R , mc^2 and β have the meanings described previously. The minimum energy T'_{th}

is specific to each unique atomic site within the specimen and is related to the bond strength and the coordination number of the atom. The behavior of the cross-section for electronic interactions with accelerating voltage is determined by the parameter β^{-2} . This dependence is illustrated in figure 2 for the case of aluminum in zeolite Y. Note that the cross-section for ionization decreases significantly with increasing accelerating voltage up to 500 kV, then levels off to a constant value.

The experimental efficiency factor, ζ , for radiolysis in silicates is 0.0001.¹⁰ That is, for every ionization event that occurs, the probability of structural rearrangement is 1 in 10,000. The cross-section for radiolytic damage is thus given by

$$\sigma_r = \sigma_e \times \zeta. \quad (3)$$

For zeolites the cross-sections for knock-on and radiolytic damage are of the same order of magnitude, and should both be considered when studying zeolites in the TEM, especially when accelerating voltages above 200 kV are used.

EXPERIMENTAL

Samples of Y zeolite (with sodium cations) with Si/Al-ratios = 2.4, 18 and ∞ and REY (with rare earth cations) with Si/Al-ratio = 3.7 were investigated. Specimens for the TEM were prepared by embedding the zeolite powder in LR White acrylic resin and thin sectioning (50-80nm) with a diamond knife on a Dupont-Sorvall MT-6000 microtome.¹¹ The specimens were stored in a dessicator to reduce the readsorption of water.

Experiments were carried out in a JEOL 200CX HREM operating between 80 and 200 kV. Incident beam current was measured at the image plane with an electrometer and the current density at the specimen was determined using $\phi_{\text{specimen}} = (\text{Mag})^2 \phi_{\text{image}}$ (ϕ =current density). This dependence was verified by measuring the current density at the image plane while maintaining a constant current density at the specimen. Over the magnification range 19,000 to 100,000, the measured current density varied inversely with the square of the magnification.

The crystalline to amorphous transformation was monitored by recording on photographic film the loss of intensity in the Bragg reflections in the selected area diffraction (SAD) pattern with time.

The SAD pattern was taken from a $5\mu\text{m}^2$ region in the center of a $20\mu\text{m}^2$ area of uniform current density. For each specimen at every accelerating voltage, the transformation was monitored several times to insure the reproducibility of the data. The dose to vitrification was calculated by multiplying the current density by the total time of exposure.

RESULTS AND DISCUSSION

The dose to vitrification is plotted as a function of accelerating voltage for the three samples containing sodium cations in figure 3. For all samples, increasing the accelerating voltage improves their radiation tolerance. This indicates that the damage is radiolytic and that knock-on damage is not significant up to 200 kV accelerating voltage. The difference between the dose to vitrification for the samples with Si/Al-ratios 2.4 and 18 is about 25%; for the sample with Si/Al = ∞ , the dose to vitrification is 3.5 and 5 times greater than that for the samples with Si/Al-ratios 18 and 2.4, respectively. Total replacement of all the aluminum by silicon produces a zeolite that is significantly more stable to electron irradiation.

Radiolytic degradation of SiO_2 in the TEM has been explained as the weakening of Si-O bonds by the incorporation of H_2O in the structure.⁹ If this mechanism is responsible for degradation of zeolites then the increase in dose to vitrification with Si/Al-ratio should be explained by the different cross-sections for radiolytic damage for Si and Al in the zeolite structure. Using equation 2, the ratio of the radiolytic cross-sections for an all Si containing zeolite versus an all Al containing zeolite is $\frac{\sigma_{\text{Si}}}{\sigma_{\text{Al}}} = 0.80$. This predicts that a zeolite structure containing only aluminum atoms (all silicon atoms replaced with aluminum atoms) should degrade with a dose to vitrification 80% that for degradation of the same zeolite containing only silicon atoms (all aluminum atoms replaced with silicon atoms). This does not explain the data shown in figure 3, where the sample containing 29% Al (Si/Al=2.4) has a dose to vitrification 20% that of the Si/Al= ∞ sample.

The data in figure 3 indicate that the mechanism and therefore the efficiency of radiolytic damage in zeolites is different from that in quartz. The important difference with aluminum in the structure is that each Al has a cation associated with it to balance the framework charge. This cation facilitates a different mechanism for the degradation of aluminum-containing zeolites.

Figure 4a shows Al tetrahedrally coordinated to four oxygen atoms in the zeolite framework. When one Al-O bond is broken (fig. 4b), the Al can remain coordinated to only three oxygens and the cation can bond to the fourth oxygen. The Al is stable with three bonds and the cation is still near it for local charge neutrality, but now the structure is permanently changed.

This mechanism explains why zeolite structures are less electron beam sensitive when dehydrated in vacuo,¹ when sodium ions are exchanged by larger cations,² or when the Si/Al-ratio is increased. At an aluminum site the larger the cation, the slower its movement into the proper position to bond to the dangling oxygen due to steric hindrance, and the greater the probability for reforming the original Al-O bond and preserving the structure. The stability of a zeolite should improve when the number of cations in the structure is reduced by using cations with greater ionic charge. Rare earth cations such as La³⁺ are strongly stabilizing due to their large size and charge, see figure 5. Adsorbed water in the zeolite structure can fill the role of a cation in the damage mechanism; thus, dehydrating the zeolite enhances its stability under the electron beam. As the Si/Al-ratio increases the number of possible degradation sites decreases and the zeolite is more stable to electron irradiation.

COMPUTER IMAGE SIMULATION

Introduction

The effects of radiolytic damage of Y zeolites on their high resolution electron microscope images is investigated using computer simulation. The goal is to determine how much of a specimen can be damaged without serious detrimental effects to the image. The high resolution images are computed using the 81D version of the Simulated High Resolution Lattice Image (SHRLI)¹² programs running on the LBL VAX8600; the dynamical electron scattering calculation uses the multislice method.¹³

3.2 Computations

Images were simulated for Y zeolite oriented with the electron beam down the [110] zone axis parallel to the channels. The atomic coordinates of Y zeolite were taken from work by Baur.¹⁴ To reduce the computation time and since the difference in the scattering potential between Al and Si is negligible, the structural model used for Y zeolite was a framework consisting of silicon and oxygen atoms without cations or water molecules.

To simulate damage in the crystal an amorphous computational cell was created by randomization of the atoms in Y zeolite. Placement of all atoms was such that the interatomic distance between atoms was at least as large as their interatomic spacing in zeolite Y.¹⁵

Dynamical electron scattering is used to simulate HREM images; the interactions of all diffracted beams enter into the calculations to produce the final electron wavefield at the bottom of the crystal. The number of diffracted beams used in the calculations must be sufficiently large to account for this dynamical scattering. For these computations 2267 diffracted beams were propagated through the crystal. In order to do this, interactions were considered with 9089 phase-grating coefficients out to 25.85nm^{-1} . For accurate representation of the phase-grating by the 128×128 array,¹⁶ the slice thickness was 0.4998nm .

Images were computed for JEOL 200CX electron microscope (EM) parameters; viz, spherical aberration coefficient of 1.2mm , spread of focus halfwidth of 10nm , beam convergence of 0.5mrad , the objective aperture corresponded to 5.0nm^{-1} and admitted 350 diffracted beams. The maximum specimen thickness assumed was 60 nm ; in general a good microtomed thin section is $45\text{-}60\text{ nm}$ thick.

Results and Discussion

Figure 6 shows the projected potential map of the Y zeolite unit cell and the amorphous computational unit cell in the $[110]$ projection. This is how the image would look using an ideal microscope with infinite resolution. In the projected potential map of Y zeolite the large ($\approx 0.74\text{nm}$) and the small ($\approx 0.22\text{nm}$) tunnels are seen clearly. The projected potential map of the amorphous cell does not show any periodicities or ordering; the structure is random.

Simulations of the HREM images of perfect Y zeolite (fig. 7, 100% perfect) at Scherzer defocus¹⁷ (-60nm for the 200CX EM) reveal that only for a specimen up to 20nm thick would the image be close to a structure image.¹⁸ In a structure image the details in the image correspond directly to features in the specimen; ie., dark areas represent a high potential, many atoms, whereas light areas correspond to few or zero atoms. A true structure image would look very much like the projected potential map viewed at the resolution of the microscope. The HREM images of the 100% perfect Y zeolite at thicknesses $10\text{-}20\text{nm}$ are not truly structure images because there are gray patches in the large tunnels

in the images. This anomalous dark contrast is due to the contrast-transfer-function (CTF)¹⁹ for the 200CX electron microscope. Figure 8 shows that the lowest frequency reflection from Y zeolite ($(\bar{1}\bar{1}1)$ in the $[110]$ orientation) is largely blocked by phase shifts in the objective lens of the microscope at -60nm defocus. Only approximately 21% of the amplitude of the $\{111\}$ reflection is passed to contribute to the image, and it is this missing frequency that produces the dark contrast at the tunnel positions.²⁰

For specimen thickness greater than 20nm at Scherzer defocus, the computer HREM images contain additional non-structural detail (fig. 7, 100% perfect). This non-structural detail results from second order interferences of the dynamically scattered electron waves.²¹ Since most microtomed thin sections are 50-60nm thick, their electron microscope images should not be interpreted intuitively because their images will bear little or no direct resemblance to their projected potential.

Figures 9 and 10 (100% perfect) show the effects of larger values of defocus on the HREM images of Y zeolite. As the microscope is defocused beyond Scherzer defocus, the image detail can not be related to the structure except for the white areas corresponding to the large channels. The large channels are visible at larger defocus values because the CTF changes shape and allows more of the amplitude of the $\{111\}$ reflection to contribute to the image.

The effects of damage on HREM images of Y zeolite are visible in figures 7, 9 and 10. The most obvious effect in the image for a specific thickness and defocus is a continuous loss of image contrast and sharpness with the loss of crystallinity. At Scherzer defocus (fig. 7) for a specimen with 60% perfect Y zeolite at a thickness 30nm or greater, the images have become fuzzy shades of grey without any discernible detail. This loss of detail with increased damage occurs for all choices of specimen thickness and microscope defocus.

In some cases the loss of detail in the image due to vitrification can be an advantage, particularly when the details are not related to the structure. A thick crystal (60nm) at a large defocus (-100nm), with 70-50% of its thickness perfect (fig. 9), produces an image which can be related to the structure. These images are similar to the images of thin crystals of 100% perfect Y zeolite at optimum defocus (fig. 7, ≤ 20 nm); both the large and small channels are visible. This is in contrast to the 60nm thick

crystal with 70-50% perfect crystal at Scherzer defocus (-60nm) which shows non-structural detail, as does a 60nm-thick 100% perfect crystal. In thick crystals at large defocus values, the amorphous damage in the specimen reduces the visibility of the non-structural detail and produces HREM images that provide information about the structure.

CONCLUSIONS

Experiments have confirmed that the damage of Y zeolites in the TEM is radiolytic and knock-on damage is not significant in the range 80-200 kV. Experimental evidence supports a model for the degradation of zeolites in which structural relaxation is enhanced at Al sites due to the presence of a cation. When an Al-O bond is broken the aluminum atom remains bound to only three oxygen atoms and the cation moves into a position to bond to the dangling oxygen atom, thus preserving local charge neutrality; however, the structure is permanently changed.

Image simulation has shown that only under very specific conditions are HREM images of Y zeolite structure images. These specific conditions are not usually met under normal experimental conditions. The limitation of specimen thickness may perhaps be reduced by ion-thinning of the microtomed thin sections. A reduction in specimen thickness will decrease the non-structural details in the HREM images which are due to second order dynamical interactions of the electron waves.

The damage of Y zeolites generally results in a decrease in the contrast and the sharpness of the details in HREM images. If a crystal has less than 20% of its thickness amorphous, its HREM images are not significantly different from those of a perfect crystal and image interpretation is unchanged. As a specimen becomes more and more damaged there is a loss of detail in the image that can in some cases be serendipitous. At large defocus values (-100nm), thick crystals (60nm) with 30-50% of their thickness amorphous, produce HREM images which can be related to the structure because the presence of the amorphous material decreases the visibility of non-structural detail. This reduction in visibility of non-structural details can aid the interpretation of the images.

ACKNOWLEDGEMENTS

The authors would like to thank Ignatius Chan of Chevron Research Company for many helpful discussions and for providing some of the samples of zeolite Y. We would like to thank Dr. M.A. O'Keefe for his help in using the SHRLI programs. Dr. R. Kilaas is gratefully acknowledged for providing the curve in figure 8.

This work was carried out at the National Center for Electron Microscopy at Berkeley and has been funded by the Director, Office of Energy Research, Office of Basic Energy Sciences, Materials Science Division of the U. S. Department of Energy under Contract No. DE-AC03-76SF00098.

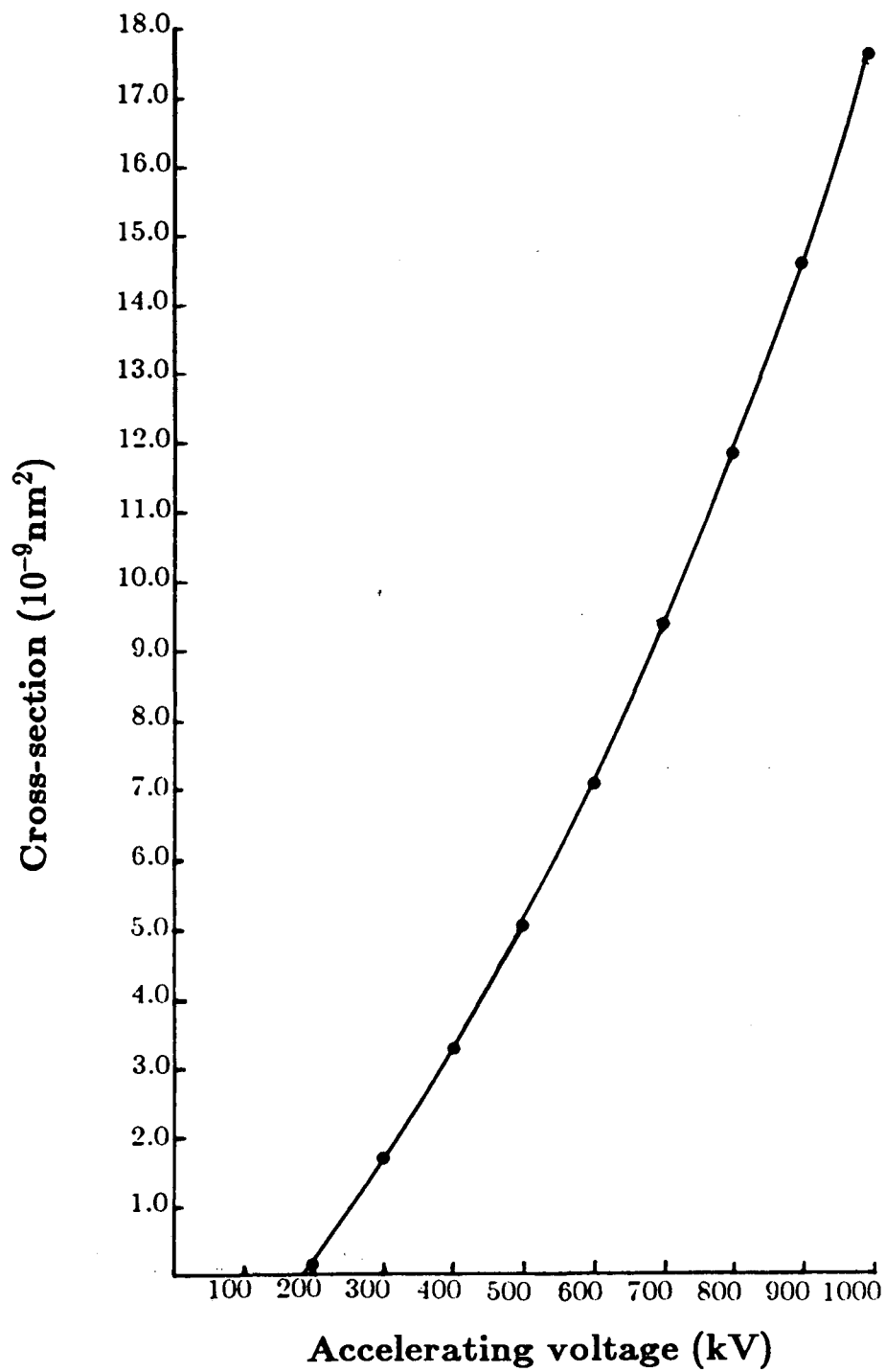
REFERENCES

- [1] Bursill, L. A., Lodge, E. A., and Thomas, J. M., *Nature* (1980) **286** 111
- [2] Bursill, L. A., Thomas, J. M., and Rao, K. J., *Nature* (1981) **289** 157
- [3] Das, G., and Mitchell, T. E., *Rad. Effects* (1974) **23** 49
- [4] Hobbs, L. W., and Pascucci, M. R., *J. Physique* (1980) **41**(C6) 237
- [5] Pabst, A., *Amer. Mineralogist* (1952) **37** 137
- [6] Pascucci, M. R., Hutchinson, J. L., and Hobbs, L. W., *Rad. Effects* (1983) **74** 219
- [7] McKinley, W. A. and Feshbach, H., *Phys. Rev.* (1948) **74** 1759
- [8] Seitz, F., and Koehler, J. S., *Solid State Physics* (1956) **2** 305
- [9] Hobbs, L. W., 'Introduction to Analytical Electron Microscopy,' ed. J. J. Hren, J. I. Goldstein and D. C. Joy, Plenum Press, New York, 1979, 437
- [10] Hobbs, L. W., *EMSA Bulletin* (1985) **15** 51
- [11] Csencsits, R., Schooley, C., and Gronsky, R., *J. Elect. Micros. Tech.* (1985) **2** 643
- [12] O'Keefe, M.A., and Buseck, P.R., *Trans. Amer. Crystallogr. Asso.*, **15** (1979) 27.
- [13] Goodman, P., and Moodie, A.F., *Acta. Cryst.* **A30** (1974) 280.
- [14] Baur, W.H., *Amer. Mineralogist* **49** (1964) 698.
- [15] Smith, J.V., in *ACS Monograph 171, "Zeolite Chemistry and Catalysis"*, (J. A. Rabo, ed.), ACS, Washington, D.C., 1976; p.17,49.
- [16] Self, P.G., O'Keefe, M.A., Buseck, P.R., and Spargo, A.E.C., *Ultramicroscopy* **11** (1983) 35.
- [17] Scherzer, O., *J. Appl. Phys.* **20** (1949) 20.

- [18] Cowley, J.M., *Ann. Rev. of Mat. Sci.* **6** (1976) 53.
- [19] Frank, J., *Optik* **38** (1973) 519.
- [20] Chan, I.Y., Csencsits, R., O'Keefe, M.A., and Gronsky, R., *J. Catal.* (in press).
- [21] O'Keefe, M.A., *Proc. 37th Ann. EMSA Meeting* (1979) 556.

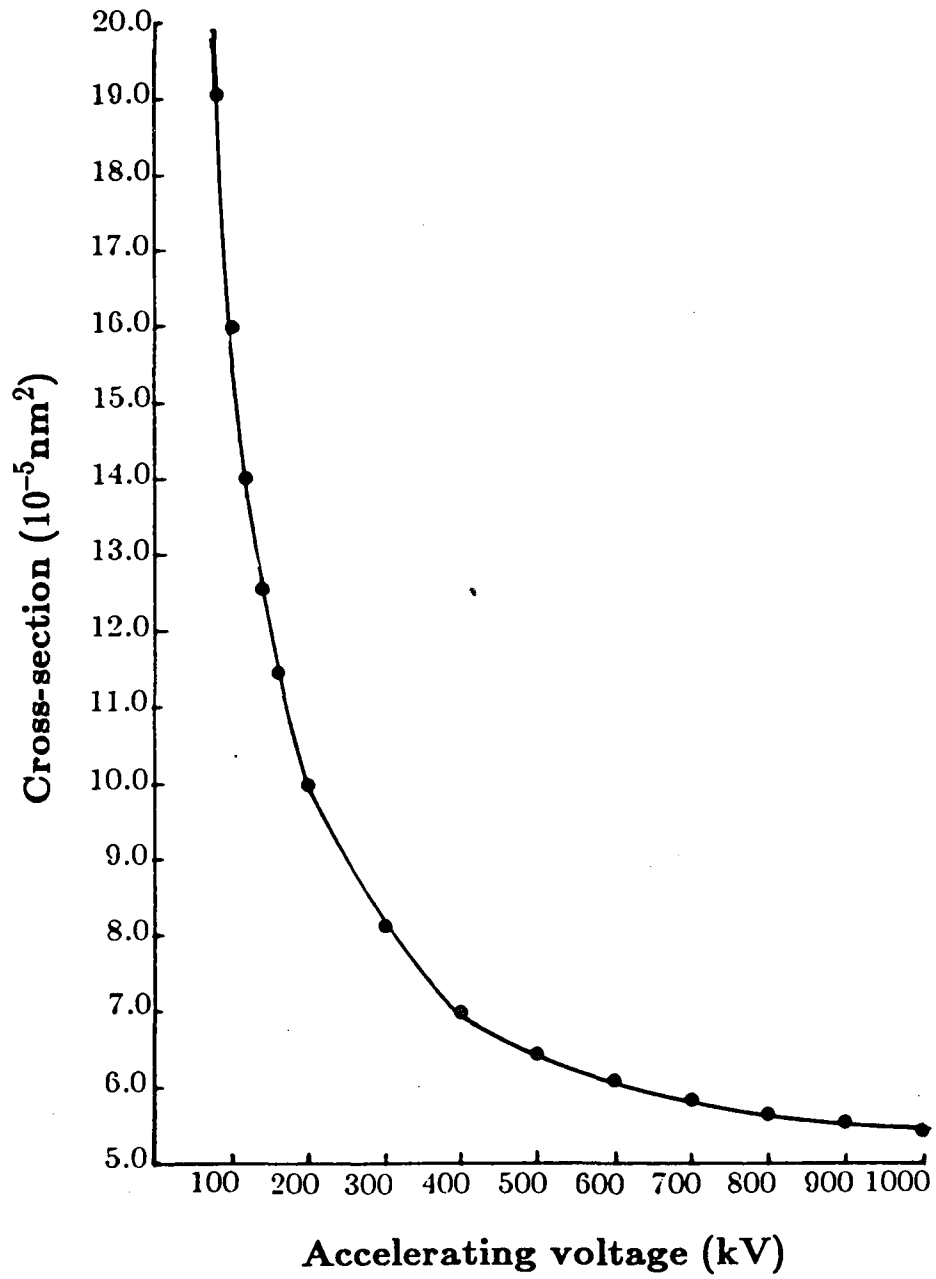
FIGURE CAPTIONS

1. Knock-on cross-section versus accelerating voltage for Al in Y zeolite
2. Radiolytic cross-section versus accelerating voltage for Al in Y zeolite
3. Dose to vitrification versus accelerating voltage for Y zeolites containing sodium cations, with $\text{Si/Al} = 2.4, 18, \infty$
- 4a. Aluminum atom tetrahedrally coordinated to four oxygen atoms in the zeolite structure
- 4b. Aluminum atom coordinated to three oxygen atoms in the damaged zeolite structure
5. Dose to vitrification versus accelerating voltage for Y zeolites containing sodium cations, with $\text{Si/Al} = 2.4, 18, \infty$ and REY containing lanthanum and neodymium cations, with $\text{Si/Al} = 3.7$
6. Projected potential map [110] for Y zeolite unit cell and the amorphous computational unit cell.
7. Computer simulated HREM images at Scherzer defocus (-60 nm) of 100%-50% perfect Y zeolite.
8. Contrast-transfer-function for the 200CX microscope at Scherzer (-60 nm).
9. Computer simulated HREM images of 100%-50% perfect Y zeolite at -100 nm defocus.
10. Computer simulated HREM images of 100%-50% perfect Y zeolite at -140 nm defocus.



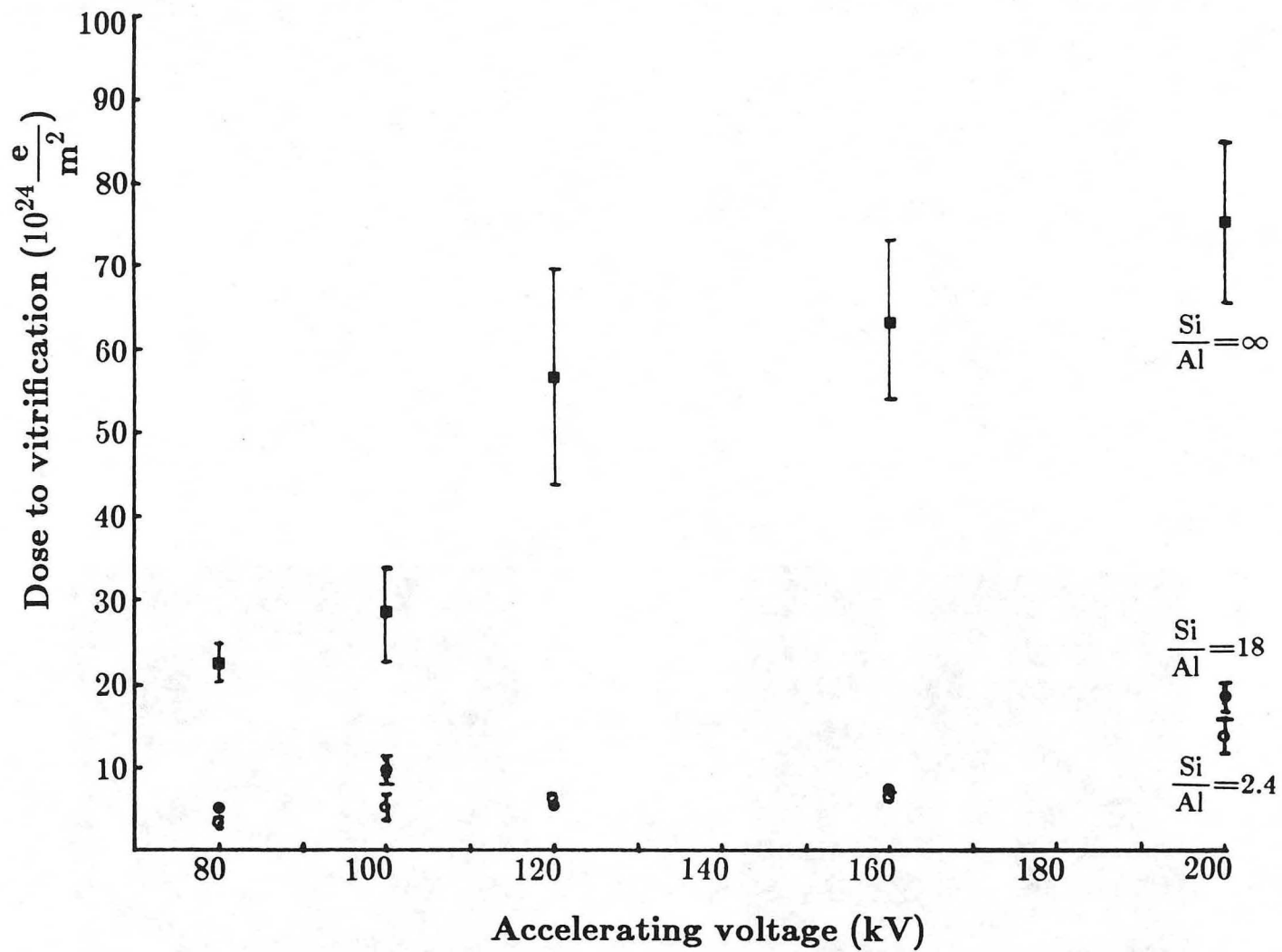
XBL 8610-3776

Fig. 1



XBL 8610-3777

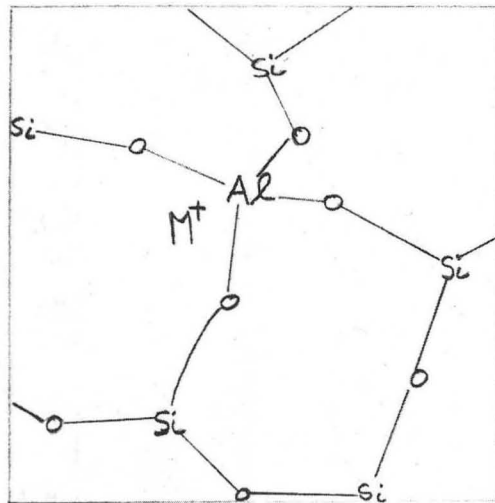
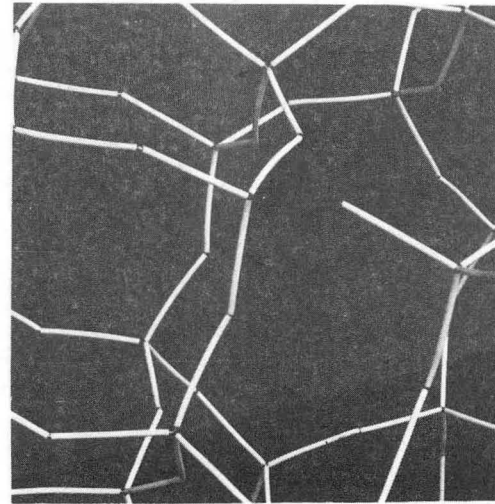
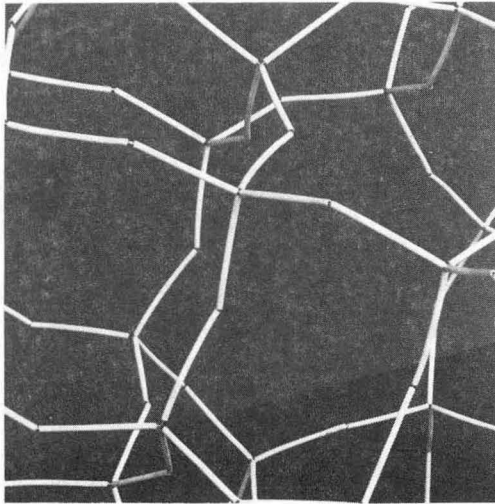
Fig. 2



XBL 8610-3778

Fig. 3

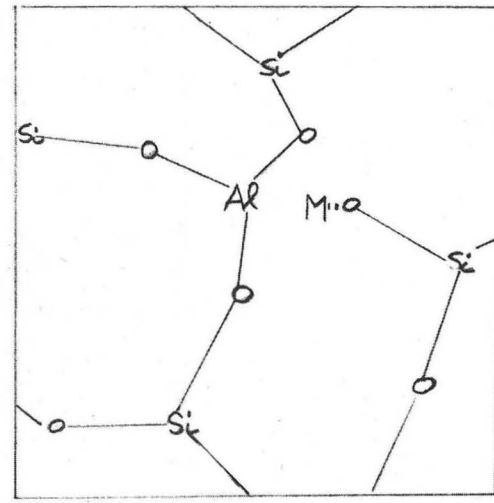
Al in zeolite



Al: 4 bonds

Cation: loosely bound

Fig. 4a



Al: 3 bonds

Cation: more tightly bound

Fig. 4b

XBB 867-5759

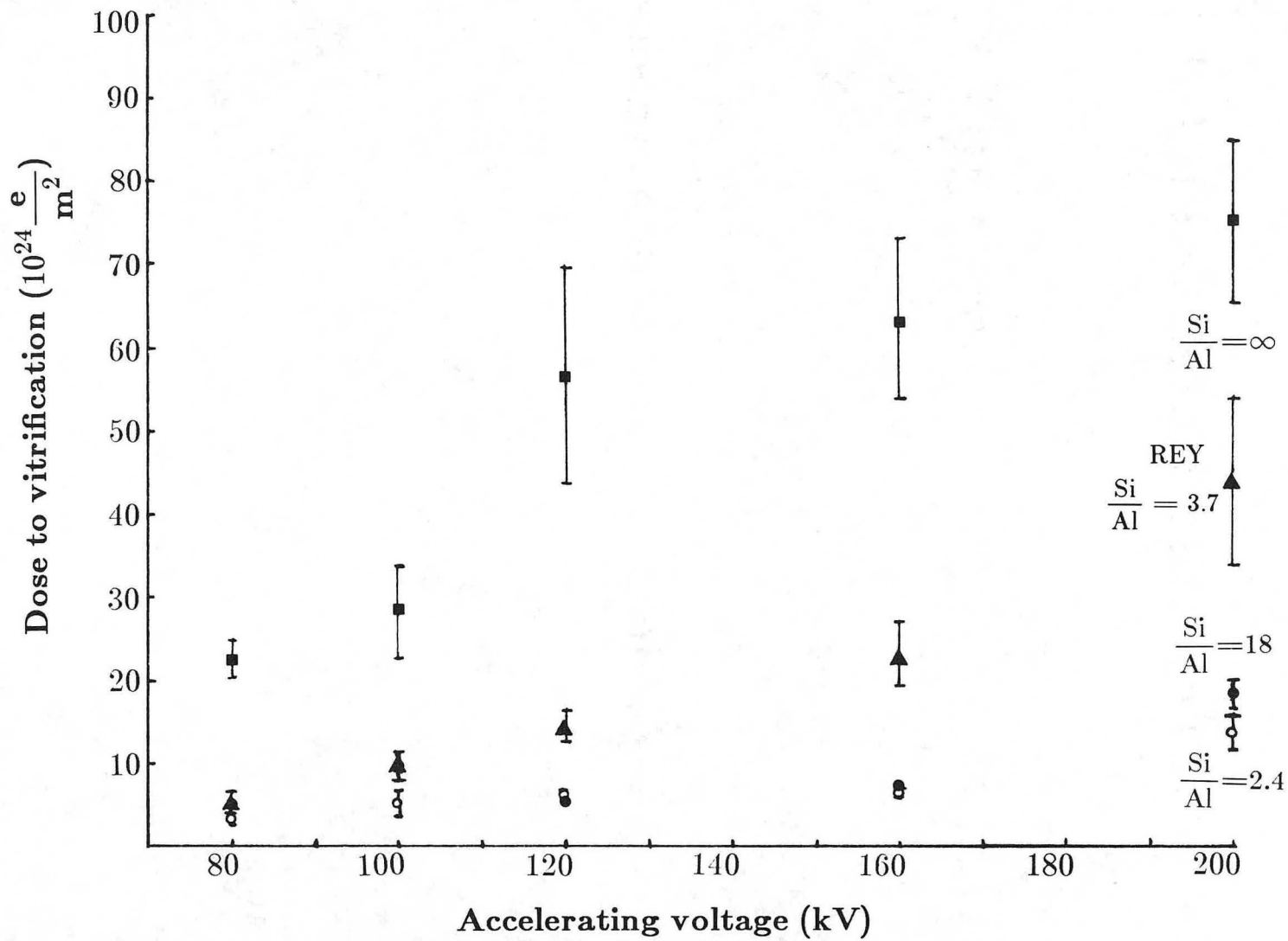
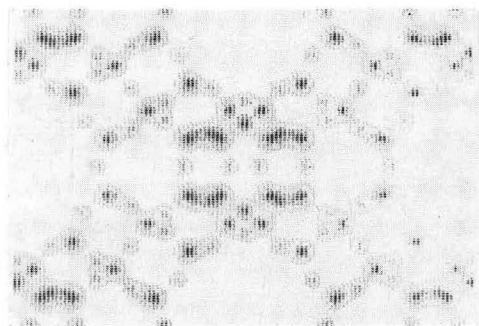


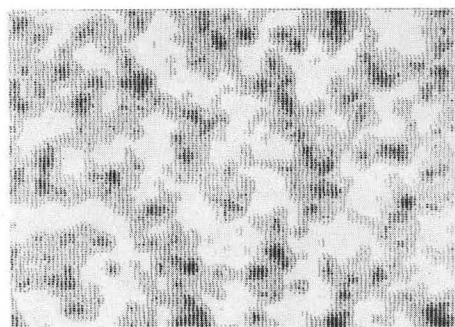
Fig. 5

XBL 8612-4979

Projected Potential [110]



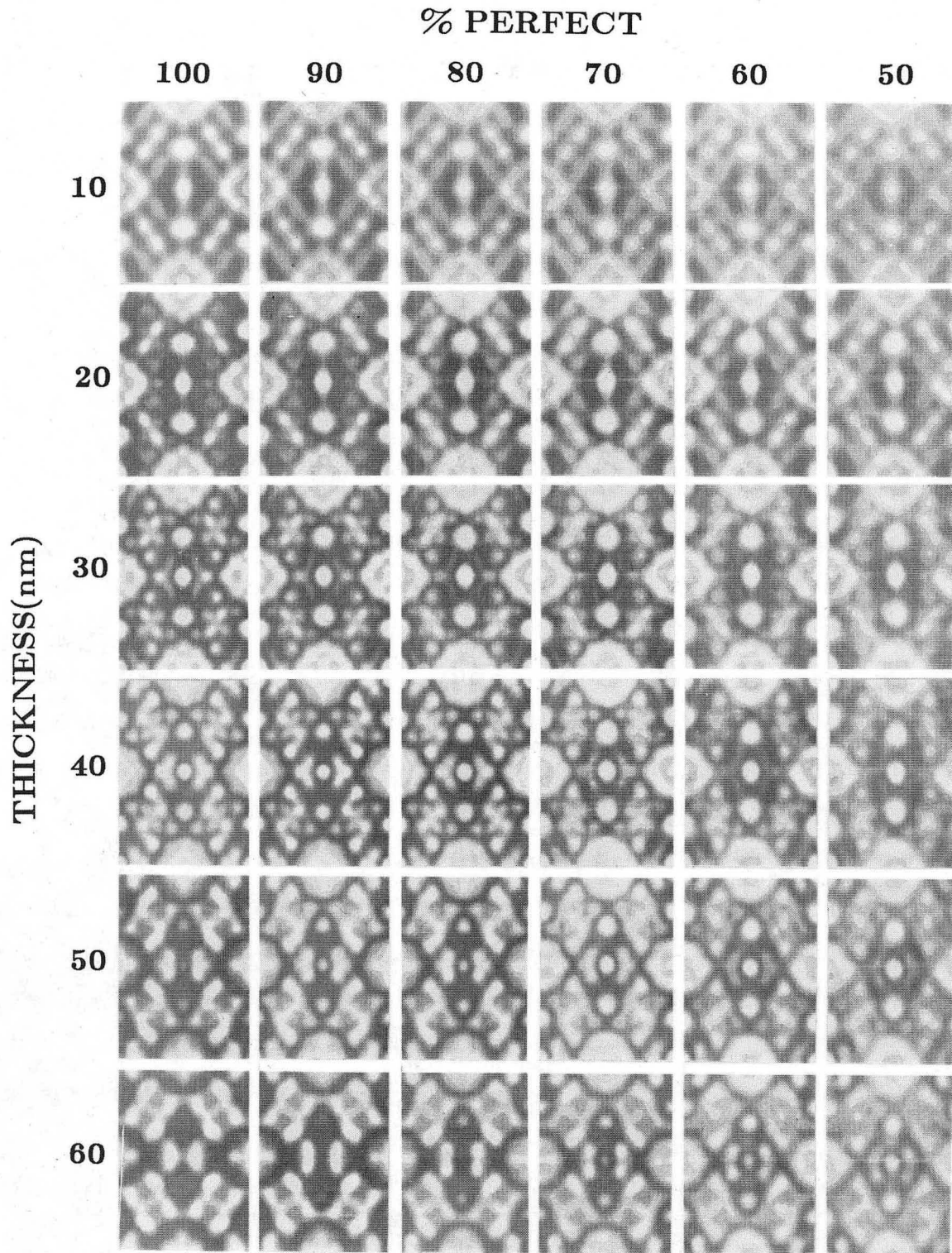
Y-Zeolite



Amorphous

XBB 850-9649

Fig. 6

$\Delta f = -60\text{nm}$ 

XBB 862-1284

Fig. 7

CONTRAST TRANSFER FUNCTION

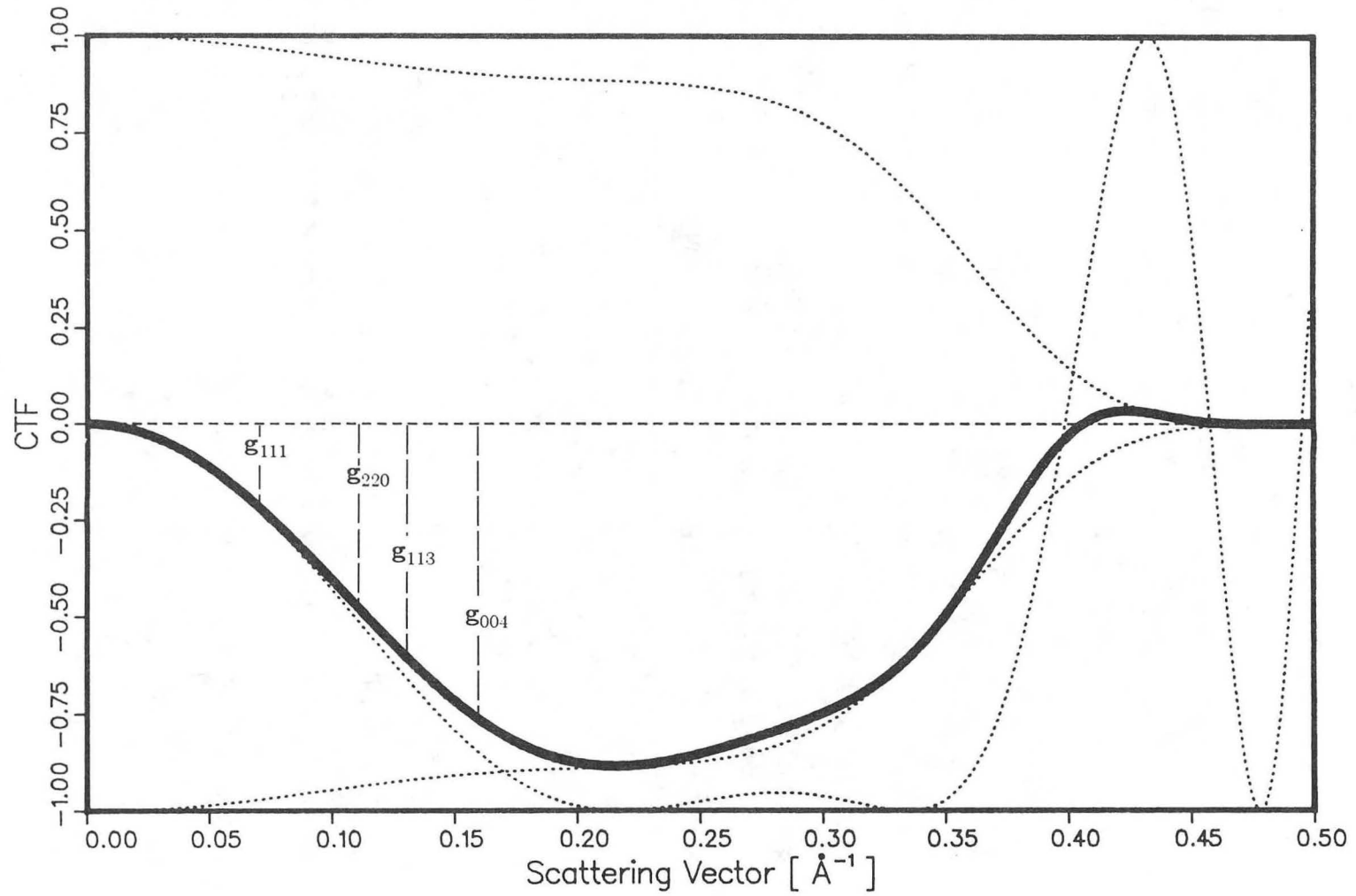
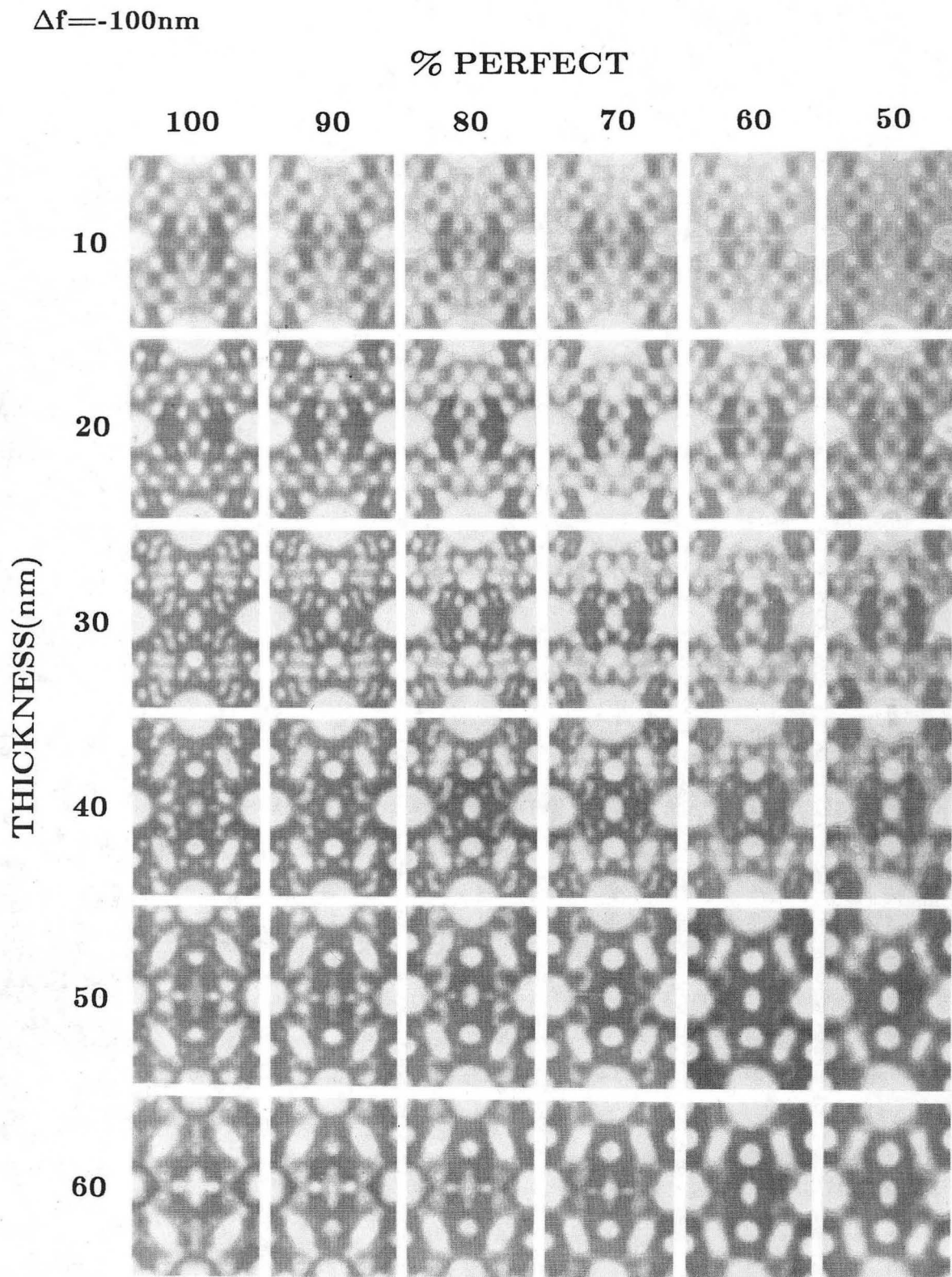


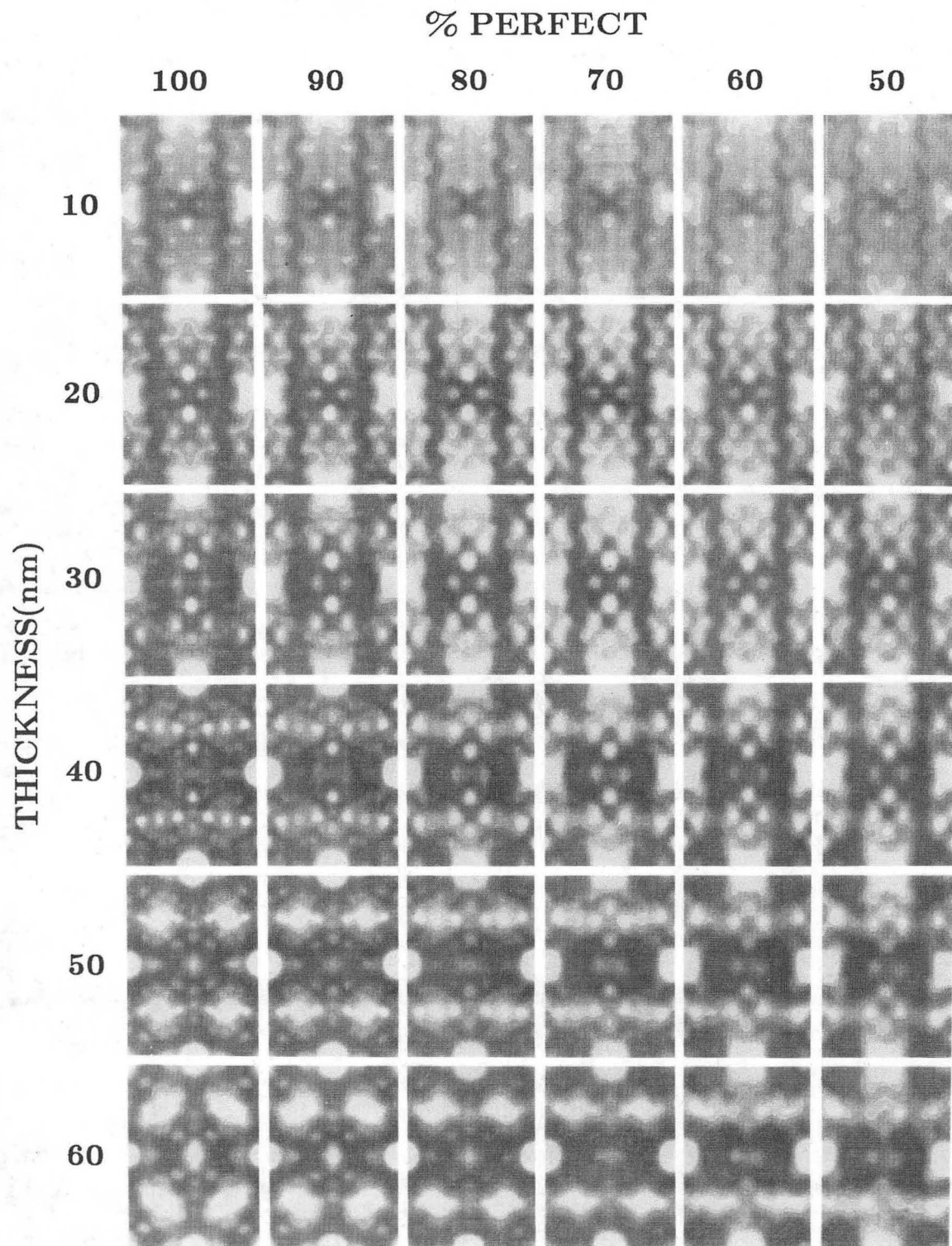
Fig. 8

XBL 862-430



XBB 862-1285

Fig. 9

$\Delta f = -140\text{nm}$ 

XBB 862-1286

Fig. 10

This report was done with support from the Department of Energy. Any conclusions or opinions expressed in this report represent solely those of the author(s) and not necessarily those of The Regents of the University of California, the Lawrence Berkeley Laboratory or the Department of Energy.

Reference to a company or product name does not imply approval or recommendation of the product by the University of California or the U.S. Department of Energy to the exclusion of others that may be suitable.

*LAWRENCE BERKELEY LABORATORY
TECHNICAL INFORMATION DEPARTMENT
UNIVERSITY OF CALIFORNIA
BERKELEY, CALIFORNIA 94720*